Next Materials 6 (2025) 100321

Contents lists available at ScienceDirect

Next Materials

journal homepage: www.sciencedirect.com/journal/next-materials

Research article

Acidic surface chemical modification of biomass combustion ash-derived activated carbon for CO_2 adsorption

Mikhail Gorbounov [a], Ludivine Hecquet-Perrot [b,c], Svetlana Ignatova [a], Peter Hewitson [a], Salman Masoudi Soltani [a,*]

[a] *Department of Chemical Engineering, Brunel University London, Uxbridge UB8 3PH, UK*
[b] *Department of Chemistry, Institut Universitaire de Technologie Paul Sabatier, Université Toulouse III - Paul Sabatier, Castres 81100, France*
[c] *Ecole Nationale Supérieure de Chimie de Montpellier, Université de Montpellier, Montpellier 34090, France*

ARTICLE INFO

Keywords:
CO_2 Adsorption
Biomass Combustion Bottom Ash
Chemically Modified Activated Carbon
Acidic Modification
NO_2 Grafting

ABSTRACT

To maximise the output and optimise a given adsorbent-adsorbate system, tailoring the material to the specific task at hand is a prominent approach. In the context of CO_2 adsorption, terminal amine groups are most common due to their exceptional affinity towards carbon dioxide. However, other methods involving introduction of alternative functionalities are often overlooked despite providing major benefits: e.g. cost-effectiveness of sorbent production and regeneration, thermal stability and etc. On these grounds, a physically activated carbon has been chemically modified with a mixture of nitric and sulphuric acid to introduce novel acidic functional groups to facilitate CO_2 adsorption. The experimental campaign was conducted by employing a randomised Box-Behnken design, evaluating the modification time and temperature as well as the ratio at which the acids (of different concentrations) have been mixed. CO_2 uptake was maximised (0.96 mmol/g at 50 °C) when treating the sorbent for 3 hours at 90 °C with 1 molar acids at a volumetric HNO_3/H_2SO_4 ratio of 1:2. Successful grafting of the nitro group was confirmed *via* spectroscopic studies, increased nitrogen content as well as other indicators. The sample was shown to possess a high working capacity, losing less than 5 % of its original uptake even after 40 adsorption-desorption cycles. As such, nitration of the surface may be viewed as a novel yet cost-effective surface modification method in the context of CO_2 adsorption.

1. Introduction

Within the realm of adsorption, there exists a sentiment that the material and the system ought to be “married” in order to maximise the benefits of the process [1,2]. As such, producing sorbents specifically for the task at hand and optimising their performance based on the target pollutant (as opposed to a generic indicator, i.e. methylene blue/iodine number or other surface area proxies) are of utter importance. Surface modification is an approach that has the potential to “tailor-fit” the sample (e.g. *via* incorporation of desired functional groups) allowing to achieve a multitude of benefits: enhance affinity towards the target molecule, increase selectivity, avoid competitive adsorption and etc. These merits are recognised by practitioners in this field and can be evidenced by the increasing prominence (just under 50 % of all adsorbent-related manuscripts focus on their modification) of such publications by the *Chemical Engineering Journal* (Fig. 1a) in the last couple of years. Yet, within the realm of CO_2 adsorption, this trend can is observed on a lower scale (Fig. 1b). This may stem from the prominence of amine-functionalisation of materials that, although immensely valuable for direct-air capture (DAC) applications, adsorb CO_2 chemically. This translates to higher enthalpies of adsorption, hence, larger regeneration energy requirements, which may (or may not) outweigh the benefits of such surface modification. As such, alternative functional groups should be studied that could bring similar benefits without (or with less) limitations.

Post-synthesis modification of the sorbent is classically done in either of two main pathways, namely, *grafting* and *impregnation*. The latter involves dispersing the modifier species along the sorbent’s surface, whilst grafting is based on chemical tethering, i.e. bonding, (as opposed to physical distribution) of the desired functionalities. The technique of physical impregnation commonly suffers from degradation (i.e. loss of modifier) upon sorbent regeneration [3]; consequently, grafting is considered to yield more stable materials, making it a more versatile strategy for adsorbent surface modification.

Generally, grafting can be categorised into two types, namely,

---

* Corresponding author.
E-mail address: Salman.MasoudiSoltani@brunel.ac.uk (S.M. Soltani).

https://doi.org/10.1016/j.nxmate.2024.100321
Received 29 April 2024; Received in revised form 26 June 2024; Accepted 16 July 2024

Nomenclature

AC	Activated carbon
ANOVA	Analysis of variance
ASTM	American society for testing and materials
ATR	Attenuated total reflection
BBD	Box-Behnken design
BET	Brunauer-Emmett-Teller
BJH	Barrett-Joyner-Halenda
CAS	Chemical abstracts service
DAC	Direct-air capture
EDS	Energy dispersive x-ray spectroscopy
FTIR	Fourier transform infrared spectroscopy
MOF	Metal-organic framework
NRMSE	Normalised root mean square error
NSS	Not statistically significant
OFAT	One-factor-at-a-time
PEI	Polyethylenimine
PFO	Pseudo-first order
PSO	Pseudo-second order
RSM	Response surface methods
SEM	Scanning electron microscopy
TEPA	Tetraethylenepentamine
TGA	Thermogravimetric analysis
VOC	Volatile organic compounds

"*grafting-on*" and "*grafting-to*" [4]. The former enhances sorption characteristics by modifying the existing surface functional groups (e.g. reduction of nitro-groups to amines or oxidation of hydroxyls to carbonyls) as can be visualised from Fig. 2a. In contrast, the "*grafting-to*" approach is mainly focused on adding desired groups to already existing functionalities. A simple example for carbonaceous adsorbents would be "opening up" sp^2 double bonds and attaching an agent with the desired functional group (Fig. 2b) to the surface of the sorbent (i.e. change from a *framework carbon-framework carbon π bond* to a *framework carbon-functional group σ bond*). To summarise, *grafting-on* alters the present functional groups (to the desired one), while *grafting-to* extends the length of the functionality's chain by adding the desired functionality.

As mentioned previously, in the remit of carbon capture, a common surface modification approach is loading of various supports with different NH_2-containing moieties. These vary greatly: from impregnation with different amines (polyethylenimine (PEI), tetraethylenepentamine (TEPA) and etc.) onto a mesoporous silica [5] or a metal-organic framework (MOF) [6], or zeolite [7] to grafting them onto different classes of adsorbents [7–12]. Regardless, such a modification would most likely facilitate increased CO_2 uptake and selectivity, which is particularly useful in DAC applications, where a sorbent with an exceptionally high affinity is required to facilitate capture from such a diluted (~420 ppm) gas stream. These cases rely on the ability of amine groups to (selectively) form carbamates as shown in Eq. 1.

$$CO_2 + 2R\text{-}NH_2 \rightarrow R\text{-}NH\text{-}COO^- + R\text{-}NH_3^+ \qquad (1)$$

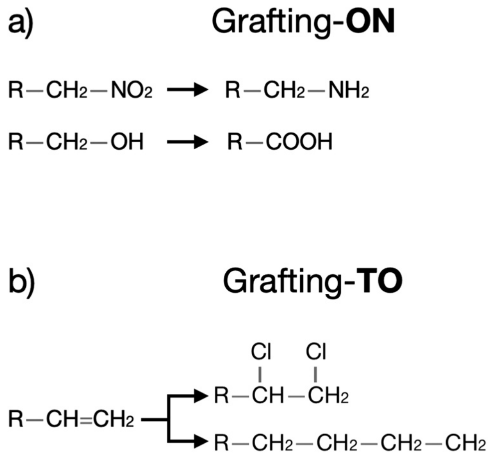

Fig. 2. Generalised examples of the a) grafting-on and b) grafting-to approaches.

In the case of activated carbons (ACs) for CO_2 adsorption, a single-step grafting procedure is less common as opposed to, for example, mesoporous silica modifications. The latter sorbent class possess terminal OH-groups, which can be readily modified with amine functionalities. For ACs, however, there may not be a sufficient number of hydroxyls to employ a single-stage process (as the high-temperature activation (especially, physical) may have diminished the volume of surface functional groups). Therefore, two-step procedures can be utilised. To start, the AC first undergoes oxidation, which is then followed by secondary treatment (e.g., with various amines [13] (including halogenated [14]), ammonia [3], etc.). As such, in the context of ACs, commonly *grafting-on* is first deployed, followed by *grafting-to*. Similarly

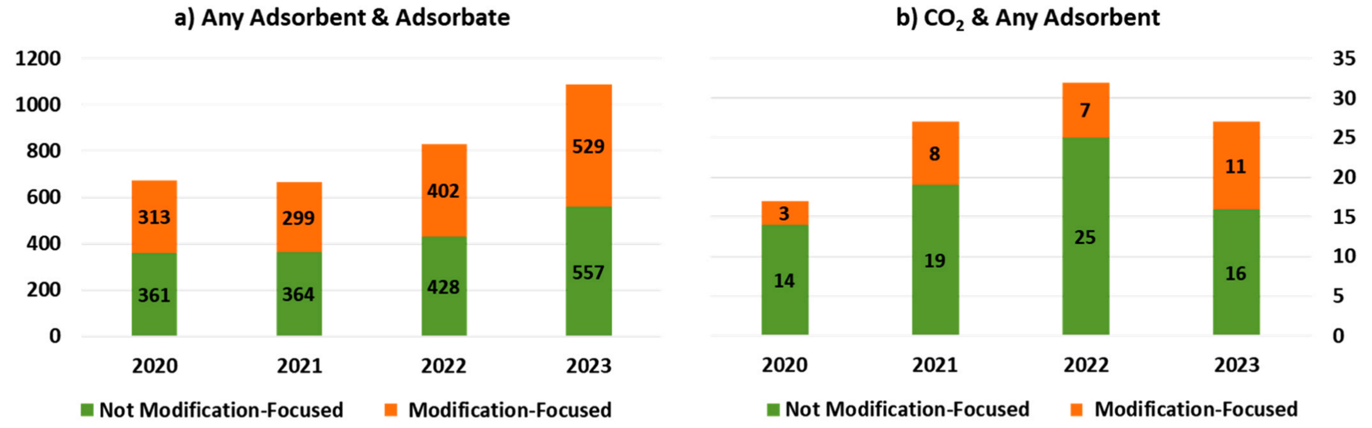

Fig. 1. Analysis of publications on the topics of a) *adsorbents and their modifications* as well as b) *CO_2 adsorption and tailored (for CO_2) sorbents* based on publications in the Chemical Engineering Journal in the timeframe of 2020 – 2023.

to other sorbents, the aim is often to generate basic surface functionalities (owing to the Lewis acid nature of the CO_2 molecule) on the surface of the AC, i.e. attach amine groups.

One approach to grafting this particular functionality onto AC involves initially oxidising the carbon surface, followed by reducing the generated acidic functional groups to amines (in step one). As such, the oxidised AC is often unfairly overlooked in the realm of CO_2 adsorption; yet it may considerably increase the capacity and selectivity of the sorbent. Moreover, by omitting the latter reduction step, a more cost-effective pathway that also aligns with environmental considerations (lack of hazardous or toxic reducing agents, e.g. $AlLiH_4$ or $NaBH_4$ [4]) can be achieved. Finally, the proposed modification technique would affect the regeneration energy penalty to a lesser extent by minimising chemisorption reactions.

Based on the above discussions, in this work a previously produced physically activated carbon derived directly (without pyrolysis) from *biomass* combustion bottom ash [15] has been chemically treated (with various mixtures of H_2SO_4 and HNO_3) to oxidise the adsorbent's surface. In existing literature, such modifications are commonly conducted utilising exclusively HNO_3 and following a one-factor-at-a-time (OFAT) methodology [14,16–18]. However, the OFAT approach does not account for potentially hidden interactions between the investigated variables. However, by employing design of experiments (DoE) techniques, an in-depth understanding of the process as well as the main effects of parameters and their interplay can readily be elucidated as scrutinised in our earlier work [19]. Additionally, improper functionalisation may affect the performance of the sorbent (e.g. *via* pore blocking) instead of improving the binding energies and selectivity over nitrogen [20] or even destroy the porous network (if modification conditions are too harsh [21]). Furthermore, many studies do not harness the potential of employing a stronger acidic agent. By utilising a mixture of H_2SO_4 and HNO_3 (also referred to as nitration mixture), firstly, a stronger extent of oxidation can be achieved while nitro-groups could be generated on the surface of the carbon.

These alternative functionalities are widely overlooked in the literature on CO_2 adsorption with main focus being drawn to basic N-containing functional groups [22,23]. However, they have previously been shown to enhance CO_2 uptakes. Functionalisation of UiO-66 with the NO_2 group, for instance, increased the adsorption capacity by ~45 % [24]. Moreover, He *et al.* showed a nitro-functionalised sorbent to outperform a carbonyl-modified analogue [25] as well as improve selectivity over N_2. Therefore, this study endeavours to modify the surface of a biomass combustion ash-based AC with various mixtures of H_2SO_4 and HNO_3 (in terms of ratios and concentrations) to maximise the CO_2 adsorption capacity of a biomass combustion ash-based AC.

2. Materials and methods

2.1. Materials

The parent material (P-AC) in this study was the physically activated biomass (white wood) combustion bottom ash-based carbon derived in our previous work [15]. The modification reagents used were H_2SO_4 (98 %; CAS 7664–93–9; Fisher Scientific) and HNO_3 (>68 %; CAS 7697–37–2; Fisher Scientific).

2.2. Selection of factors and design of experiments framework

The experimental campaign evaluated the impact of several variables, namely, a) modification temperature, b) acid mixing ratio (volumetric), c) contact time and d) the concentration of each *individual* acid within a given solution. CO_2 uptake has been selected as the response variable. The investigation was undertaken using a Box-Behnken design (BBD), comprising a total of 27 experiments (three of which were repetitions at the centre point of the design). This particular DoE framework was opted for as it allows to eschew experiments located at the edge-points of the design [19]. For this (and other nitric acid-based) campaigns avoiding simultaneous extreme points (i.e. maximum time and temperature with high acid concentrations) is advisable to minimise generation of brown gas (NO_2) since NO_2 is acutely toxic and poisonous. All experiments were conducted under a fume hood to avoid exposure to NO_2.

2.3. Preparation of chemically modified carbon

The first step of the modification process was heating of a three-necked round-bottom flask (as can be visualised from Fig. 3) containing the prescribed acid mixture (210 mL) to the desired temperature. This was achieved *via* a heating mantel as well as an air-cooled condenser (Findenser, 400 mm) to prevent evaporation of the liquid modifier. This particular type of glass reactor was selected to achieve continuous temperature measurements (neck one) and condensation of vapours (neck two, i.e. central neck), whilst leaving a (normally closed with a glass stopper) port for addition of P-AC (neck three). Upon reaching the designated temperature, 0.5 g of P-AC was introduced into the reactor, thus, commencing the contact (modification/residence) time. Through all these stages, the reaction mixture was continuously stirred at 250 rpm using a magnetic stirrer.

Subsequently, a separation step *via* a Büchner–Bunsen funnel-flask system was undertaken, where the samples were also washed with deionised water until a neutral pH was reached. The produced material was then placed in an oven for overnight drying (12 hours at 80 ºC) and characterised thereafter.

2.4. Sorbent characterisation

Thermogravimetric analysis (TGA) tests employing a Mettler Toledo TGA 2 and pure gases (namely, N_2 (N 4.8) and CO_2 (N 2.8), both procured from BOC, UK) were conducted to assess the CO_2 adsorption capacity. The programme contained a 15 min degassing/purge step at 150 °C (under 50 mL/min of N_2). This was done to ensure alleviation of any adsorbed from ambient air species off the surface of the AC. Then, the sample was brought (-10 °C/min) to the prescribed adsorption temperature, where CO_2 was introduced and maintained at a flow rate of 50 mL/min for 30 minutes. In the case of cyclic adsorption-desorption trials, after the adsorption step, the desorption step commenced following the same programme as the initial purge. The TGA was also used to conduct proximate analysis following ASTM D3172 [26]. Spectroscopic analysis, i.e. Fourier Transform Infrared Spectroscopy (FTIR), was also employed for characterisation *via* the Attenuated Total Reflection (ATR) approach using Shimadzu IRSpirit. 20 scans (4 cm^{-1}

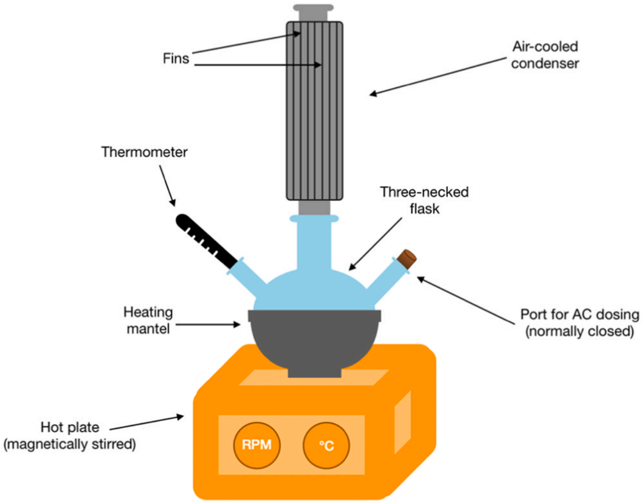

Fig. 3. Graphic representation of the glass modification reactor.

resolution) were done in the region of 600 – 4000 cm^{-1}. Scanning Electron Microscopy/Energy Dispersive X-ray Spectroscopy (SEM/EDS) were conducted on a JOEL IT200. Within that, copper plates were employed as the background material. In addition, as the carbonaceous sorbent is electrically conductive, no gold sputter coating was required. Further elemental characterisation was done *via* ultimate/CHN analysis (Flash 2000 Organic Elemental Analyzer Thermo Scientific) with acetanilide being the standard reference. Surface area was analysed based on the Brunauer-Emmett-Teller surface area (S_{BET}) measurements, i.e. N_2 at 77 K, [27] in a Micromeretics ASAP 2020 apparatus. Prior to this, the analysis chamber was degassed: 6 hours at 200 °C (at a ramping rate of 5 °C/min). Similar degassing procedure was adopted before the experiments to measure CO_2 adsorption isotherms (0 – 50 °C). The data from these experiments were used for equilibrium model fitting and isosteric heat of adsorption calculations (*via* the Clausius-Clapeyron equation).

3. Results and discussions

3.1. Modification and optimisation campaigns

In the field of organic chemistry, the HNO_3/H_2SO_4 mixture is often referred to as the "nitration mixture". Sulfuric acid protonates nitric acid (Eq. (2)) generating the extremely reactive nitronium ion (i.e. NO_2^+). As such, this mixture is preferable over pure nitric acid as the agent to introduce NO_2 groups (since pure HNO_3 mostly oxidises the surface instead of nitrating it).

$$HNO_3 + 2H_2SO_4 \rightarrow NO_2^+ + H_3O^+ + 2HSO_4^- \tag{2}$$

Since carbon-based adsorbents possess an aromatic nature (as depicted in Fig. 4), it is believed that once functionalised their properties resemble those of the analogous aromatic hydrocarbon [21]. Therefore, nitration of AC is believed to follow the mechanism of electrophilic aromatic substitution [28], as shown in Fig. 4. Once grafted, the nitro group is believed to attract the electron-deficient (δ+) carbon atom of CO_2 *via* electrostatic forces [23].

However, even for the HNO_3/H_2SO_4 mixture, nitration may be transient and oxidation can still occur, especially in the cases of excessively prolonged contact time [29]. This aspect highlights the importance of optimisation of modification time as part of the potentially impactful variables as well as the value of optimal modification envelope identification. Therefore, the modification temperatures and times coupled with the ratios of acids within the nitration mixture as well as the individual acid concentrations within each modifying agent formulation, are presented in Table 1.

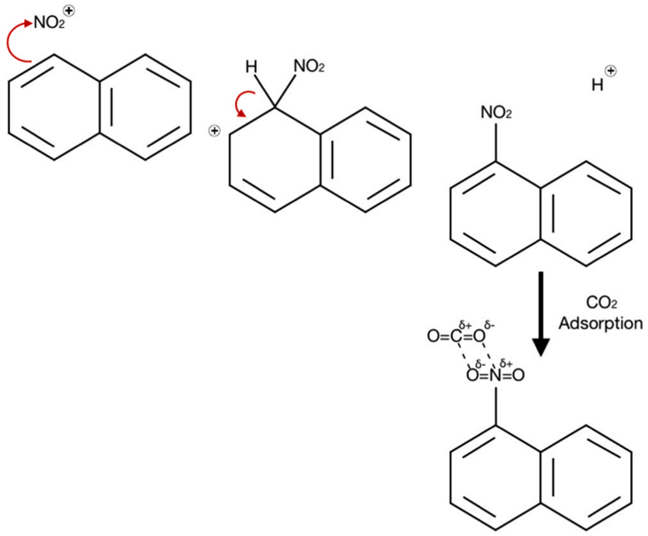

Fig. 4. Nitration mechanism of a carbonaceous sorbent as well as the attraction mechanism between the CO_2 and the sorbent with the grafted NO_2 group.

3.2. Statistical analysis and significance of results

The experimental campaign was executed based on an experimental design produced by Minitab (version 18). The randomised trials were conducted and the CO_2 adsorption capacities of all of the produced samples were analysed as the response variable, and employing analysis of variance (ANOVA), as well as Response Surface Methods (RSM). The outcomes of this are presented in Table 2 (and Fig. 5), elucidating which factors were found to be most impactful and which were not statistically significant (NSS).

The model results ($R^2 = 0.911$, adjusted R^2 of 0.808, and a predictive R^2 of 0.499) presented in Table 2 indicate that only the individual acid concentrations and the modification temperature were statistically significant, following the literature-standard criterion of p-values < 0.05. Despite being a somewhat arbitrary and subjective value [30,31], the p-value is believed to signify a 5 % chance of error in attributing the observed effects to the proposed interaction/factor, i.e. a 95 % confidence in its statistical significance. The robustness of this selection criteria for significance, however, is supported by the "2σ rule" which suggests approximately 95 % of values to fall within two standard deviations from the mean of the examined dataset. As such, only the reaction temperature and the concentration of the acids are considered to have had a statistically significant impact on CO_2 uptake. Within this, due to the extremely low p-values, the effects are believed to be backed by strong evidence [32] and, due to high F values, can also be deemed pronounced.

Further, the analysis presented in Table 2 may tempt to consider the interaction between the mixing ratio and acid concentrations as "*nearly*" statistically significant. Alternatively, a "*significance in 90 % of cases*" may be opted for allowing this interaction to surpass the threshold. These practices (as well as evaluating an abundance of responses to increase the likelihood of model/parameter significance on a given output and etc.) are frowned upon and are commonly referred to as "*p-hacking*". These and other aspects (e.g. selective reporting, misrepresentation) are elaborated on in [33]. Hence, adhering to the 0.05 p-value threshold for statistical significance is recommended, and adopted by the authors in this work.

A further output of the model that facilitates a better visualisation of the examined design space are the contour plots, as depicted in Fig. 5.

As depicted in Fig. 5, the CO_2 uptake appears to increase towards the edge-points of the design space. However, given the absence of experimental points at the corners of the framework (the stand-out feature/limitation of BBD), these have to be estimated and extrapolated and may not as representative and accurate the internal volume of the design. As such, BBD-based models often point towards the edges as the optimum conditions, and the case of the chemical modification outlined above was not an exception. However, this was, indeed, the case in this work based on a verification experimental trial that confirmed successful optimisation of this operating envelope. The optimum point that maximised the material's CO_2 adsorption capacity was found to be at the maximum studied temperature (90 °C) and time (3 h) whilst employing the minimum acid ratio (1:2) and minimum concentration (1 M). These conditions led to a material yield of ~79 wt%.

Prior work indicated using lower acid mixing ratios could increase

Table 1
The investigated factors and their levels studied via the box-behnken design.

Factors	Levels		
Time, h	1	2	3
Temperature, °C	30	60	90
HNO_3/H_2SO_4 Ratio (vol)	1:2	1:3	1:4
Concentration, M	1	6	11

Table 2
Results of ANOVA for the modification experimental campaign.

Factors	F-Value	p-Value	Significance
Time	2.63	0.131	NSS
Temperature	57.01	0	1
Acid Ratio	3.26	0.096	NSS
Concentration	43.3	0	2
Time*Time	0.83	0.379	NSS
Temperature*Temperature	1.61	0.229	NSS
Ratio*Ratio	0.66	0.433	NSS
Concentration*Concentration	3.37	0.091	NSS
Time*Temperature	0.67	0.43	NSS
Time*Ratio	1.35	0.268	NSS
Time*Concentration	0.1	0.753	NSS
Temperature*Ratio	1.29	0.278	NSS
Temperature*Concentration	0.19	0.67	NSS
Ratio*Concentration	4.47	0.056	NSS

CO_2 uptake due to a larger N-content of samples [28]. Additionally, extending treatment time and temperature may more effectively dissolve ash impurities (present in P-AC) consequently leading to higher specific adsorption uptakes. Moreover, lower acid concentrations are associated with generation of nitro groups rather than O-heteroatom-based groups (e.g., keto, hydroxy, etc.) [34,35]. The NO_2 functionality is more polar than C═O [23], hence, providing a more electrostatically robust surface that may attract more CO_2 molecules. As such, the optimally modified (90 °C, 3 h, 1 M, HNO_3:H_2SO_4 ratio of 1:2) edge-point sample was labelled as AC-Mod and taken for extensive characterisation.

3.3. *Characterisation of the optimum sample (AC-Mod)*

3.3.1. *SEM/EDS*

AC-Mod underwent examination using Scanning Electron Microscopy (SEM). The resulting images of AC-Mod are shown in Fig. 6.

Similar to the parent AC, AC-Mod exhibits substantial heterogeneity and surface roughness, which is expected of waste-derived carbonaceous adsorbents. The shard-like form is also attributed to their amorphous nature. The performed acidic modification did not significantly change the surface morphology of the sample as it was intended to chemically adjust its surface by grafting functional groups. In order to examine the surface elemental composition of AC-Mod, Energy Dispersive X-ray Spectroscopy (EDS) was conducted.

As indicated in Table 3, the acidic treatment has induced changes in the material compared to P-AC [15]. Notably, sulphur-containing moieties, albeit in only 0.1 % by mass, have been detected on the surface of AC-Mod (P-AC did not present a surface S-content). These may have persisted despite washing with deionised water. Interestingly, no elemental N has been identified on the surface of AC-Mod. This absence could be attributed to the limitations of this analytical technique: characterising only surface (and not bulk) elemental composition, and, secondly, struggling to accurately quantify elements with a low atomic mass (<23 amu of sodium) [36]. In order to address this issue, CHN (ultimate) analysis was performed to determine the N and C contents of AC-Mod. The inorganic elements (namely, Ca, Si, Al) found as part of the sample persist from the ash precursor. Notably, no Mg or K as well as a lesser amount of calcium have been observed, suggesting the acidic modification to have also purified the material *via* dissolution of some inorganic species. These materials may also have an influence on the CO_2 adsorption capacity of the material mainly by changing the charge distribution along the surface of the adsorbent. To accurately quantify them, however, a bulk technique, such as proximate analysis, is preferred.

3.3.2. *Ultimate analysis*

Ultimate analysis has been utilised to quantify the lighter elements (namely, carbon, nitrogen and hydrogen) as part of the bulk of AC-Mod with corresponding data is presented in Table 4.

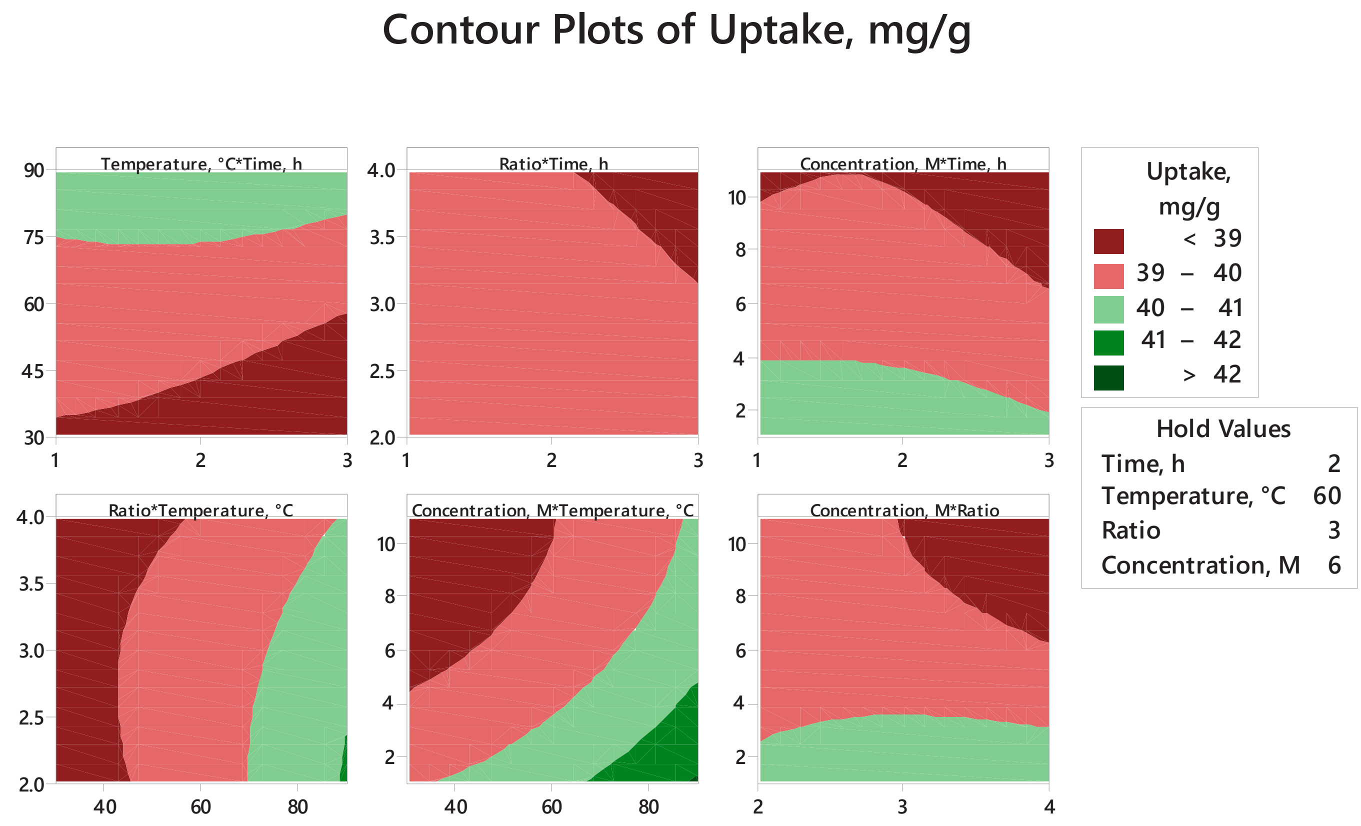

Fig. 5. Contour plots of CO_2 uptake vs examined factors.

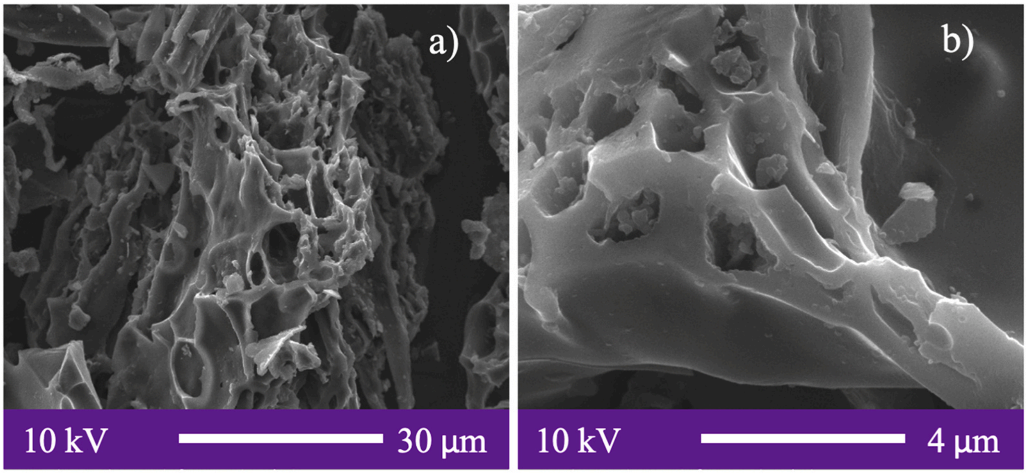

Fig. 6. SEM images of AC-Mod.

Table 3
Surface elemental composition of AC-Mod and P-AC acquired via EDS.

Element	Weight %	
	P-AC	AC-Mod
C	26.7	77.6
O	72.0	21.3
Ca	0.6	0.4
Si	0.3	0.4
Al	0.2	0.2
S	0	0.1
Mg	0.1	0
K	0.1	0

The modification of the carbon led to a non-negligible rise in N-content, specifically from 0.26 % [15] to 1.43 % (i.e. a 5.5-fold increase). This elevation is attributed to the presence of nitrogen-containing surface functionalities stemming from the treatment with the nitration mixture. Furthermore, increases in carbon and hydrogen content (P-AC exhibited 54.47 % and 1.00 %, respectively [15]) may arise from the dissolution of ash due to the acidic treatment. This hypothesis is supported by the EDS results (Section 3.2.1) that show presence of inorganic species on the surface. Yet, an alternative bulk quantification technique, i.e. proximate analysis, is preferred as a more reliable method.

3.3.3. *Proximate analysis*

Proximate analysis [26] was employed to assess the produced sorbent in terms of bulk composition, namely, quantification of moisture, volatile organic compounds (VOC), fixed carbon and ash contents.

According to Table 5, AC-Mod exhibits a moisture content of 7.2 %, significantly more than the parent material (1.5 %). This discrepancy may suggest that the modified sample has a greater affinity for moisture than the parent material as the H_2O was most likely adsorbed from ambient air. This is in-line with the hypothesis of polar functionalities serving as points of attraction for the H_2O molecule *via* hydrogen bonding [22]. Yet, the nitro group is less polar than the amine group [23], which may serve as a benefit in terms of competitive adsorption with water vapours present in air or flue gases (for the purposes of DAC and post-combustion capture applications, respectively).

Table 4
Ultimate analysis results of AC-Mod and P-AC.

Element	Weight %	
	P-AC	AC-Mod
C	54.47	65.45
H	1.00	1.38
N	0.26	1.43
Other	44.27	31.74
Reference	[15]	This work

Table 5
Proximate analysis results of AC-Mod and P-AC.

Sample name	Moisture, wt %	VOC, wt %	Fixed C, wt%	Ash, wt %	Reference
AC-Mod	7.2	21.3	58.4	13.1	This work
P-AC	1.5	7	49	42.5	[15]

Additionally, there is an observed increase in VOCs, rising from 7 % to 21.3 %. This may stem from a rise in number of volatile functionalities on the surface of the AC as a result of the modification (i.e. nitration and/or oxidation). This is corroborated by the greater C, H and N values (all would contribute to the rise in VOC content) as evidenced by the ultimate analysis. Simultaneously, a decline in ash content is noted. This is believed to be caused by various reactions between some inorganic ash impurities and the employed acids. Resulting in water-soluble salts that have been alleviated from the bulk of the sorbent during the final washing step. As such, this modification may also serve as a purification treatment, providing an additional benefit to this approach.

Finally, all of these aforementioned changes affect the resulting fixed carbon content. Therefore, no conclusive statements can be made as to the changes to the carbon matrix based on the data from Table 5. As such, further characterisation is required to envisage the full impact of the modification onto the sorbent.

3.3.4. *Spectroscopic analysis*

3.3.4.1. Fourier-transform infrared spectroscopy. The FTIR spectrum of AC-Mod (Fig. 7) supports the hypothesis of successful oxidation and nitration, as evidenced by the presence of O-H (3192 cm^{-1}) and N-O (1557 cm^{-1}) stretching as well as O-H bending (1399 cm^{-1}) vibrations [37], since the parent AC lacked these bonds. According to the literature, in surface treatment with pure nitric acid, oxidation with higher concentrations of HNO_3 tends to favour the development of carbonyl (and then carboxyl) functionalities [34]. On the other hand, lower HNO_3 concentrations allow for the persistence of nitro groups [35]. The spectrum of AC-Mod aligns well with this hypothesis since a 1 M solution was employed as the result of the DoE optimisation.

Furthermore, the FTIR spectrum reveals the presence of skeletal C=C bonds at 1652 cm^{-1} [15] as well as stretching vibrations of C-H at

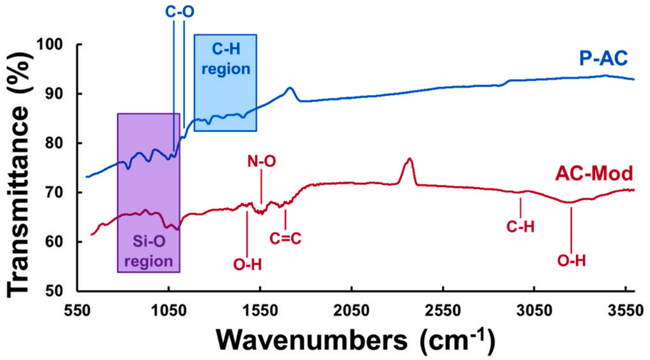

Fig. 7. Infrared spectra of AC-Mod (red; bottom) and P-AC (blue; top).

2959 cm^{-1} [37]. Finally, the observed Si-O peaks (at wavenumbers of 1019 and 1080 cm^{-1} [15]) are associated with the remnants of ash species as part of the sorbent (consistent with FTIR spectrum of P-AC).

3.3.4.2. Raman spectroscopy. As a complementary (to FTIR) characterisation technique, Raman spectroscopy was also deployed. This analysis method allows to discern between ordered/graphitic (or sp^2-hybridised) and disordered/diamond (or sp^3-hybridised) carbon atoms *via* the G and D band peaks, respectively [38]. Based on the spectrum presented in Fig. 8, the I_D/I_G ratio (i.e. D band to G band intensity ratio) is estimated to be 0.72, representing an ~12 % decrease compared to the P-AC. This observation is somewhat unexpected. It was reported that the I_D/I_G ratio is highly dependent on treatment time (exhibiting a non-linear relationship), albeit for carbon fibres treated at 60 °C with a concentrated HNO_3/H_2SO_4 mixture at a volumetric ratio of 1:3 [29]. However, in those cases, an increase in the D-band was noted. The unexpected decrease observed in this study may be attributed to the use of a parent material with high surface heterogeneity, (based on the Raman spectroscopy and porosity analysis of our P-AC [15]), hence, large D band peak intensity and I_D/I_G ratio, unlike the pristine (i.e. non-activated) fibres in the study of Zhang *et al.* [29], which do not possess large amounts of surface defects.

Alternatively, the produced functionalities could have absorbed some of the incident light assuming they are located at the more easily accessible edges and defects of the graphene sheets. This would hinder inelastic (Raman) scattering of the "defective" carbon atoms leading to a drop in intensity of the associated D-band. Supporting this theory is the fact that the produced functionalities, namely nitro and hydroxyl, would not be prominently displayed on Raman spectra as a distortion of the electron cloud around the atoms is required [39], resulting in the absence of polar groups (hydroxyl and nitro) in Fig. 8.

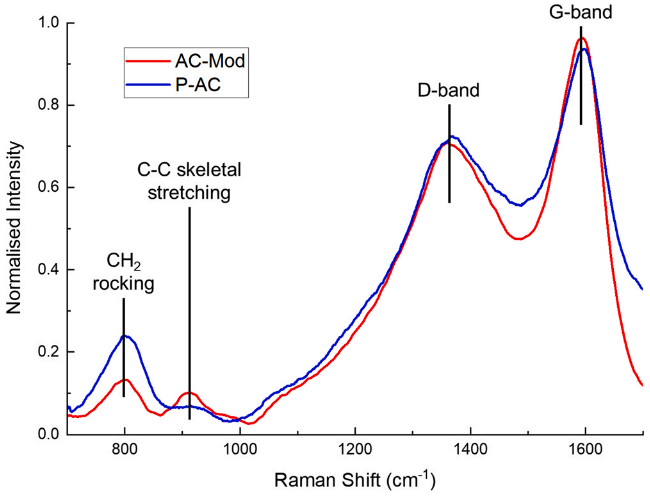

Fig. 8. Raman spectra of AC-Mod (red) and P-AC (blue).

Furthermore, C-C skeletal stretching as well as CH_2 rocking peaks have been observed at Raman shifts of ~879 cm^{-1} and ~775 cm^{-1}, respectively [40]. Additionally, the bigger depth of the troughs between the D and G bands for AC-Mod could probably be associated with enhanced dispersal of the amorphous and graphitic phases. This may be the result of the removal of the ash impurities during acidic modification process.

3.3.5. Surface area analysis

Analysis of the surface of AC-Mod elucidated further changes as a result of modification. AC-Mod exhibits a type IV isotherm and a hysteresis loop similar to the parent material. Yet in Fig. 9, the adsorption and desorption branches of the BET physisorption isotherm of AC-Mod do not meet at lower relative pressures, displaying an open hysteresis curve. This phenomenon can be attributed to "pore swelling" [41], which involves deformation of the shape (and a rise in volume) of the pore [42]. The carbon scaffold may suffer permanent damage as a result of the polyaromatic structure of an AC collapsing, trapping gas molecules as part of the adsorbent [43]. This underscores the significance of cyclic adsorption-desorption studies (Section 3.2.6.5).

Alternatively, an open hysteresis loop could also be caused by chemisorption of adsorbate [41], but for N_2 adsorption isotherms, pore swelling would be a more plausible explanation due to the inherently physical nature of the interaction between nitrogen and ACs.

Compared to the parent AC, two other notable observations can be made, namely, a lower inflection point as well as total uptake. The latter is responsible for the decrease in S_{BET} (221 m^2/g compared to 248 m^2/g for P-AC); whilst the reduced initial sharp increase stems from a lower t-plot micropore volume (0.0633 cm^3/g compared to 0.0936 cm^3/g). This outcome is largely anticipated since surface modification increases the possibility of pore blockage by the generated functionalities, causing reductions in both of these values. This hypothesis can be further backed up by investigating the pore size distribution following the Barrett-Joyner-Halenda (BJH) model (using the desorption branch) as presented in Fig. 10.

Within this, the average pore diameter is found to be 3.6 nm, maintaining the same value as P-AC. As such, the described acidic modification did not facilitate production of further porosity. It has mostly enhanced the surface electrostatic properties, which have influenced adsorption of not only N_2 but also CO_2.

3.3.6. CO_2 adsorption experiments

The efficacy of surface acid modification has also been evaluated based on the interaction between AC-Mod and CO_2.

3.3.6.1. Adsorbent's microstructure analysis. Apart from the N_2 isotherm at −196 °C, a CO_2 isotherm at 0 °C has also been deployed as this method is preferred for characterisation of micropores due to a) lack of adsorbate diffusion limitations arising from the cryogenic temperatures [44] and b) the lesser kinetic diameter of the CO_2 molecule. These benefits allow for a more accurate determination of the adsorbent's micropore structure presented in Fig. 11.

Their similar shapes suggest that the modification did not generate new porosity (corroborating the hypothesis from Section 3.2.5). On the other hand, the larger micropore volume of AC-Mod compared to P-AC has been noted. This may stem from the ash dissolution, which, in turn, leads to the greater microporosity and dictates enhanced adsorption performance of the sample. Additionally, these results highlight the value of CO_2 adsorption at0 °C tests for micropore analysis as opposed to nitrogen at −196 °C isotherm.

3.3.6.2. Adsorption capacity. CO_2 adsorption on AC-Mod follows the expected physisorption trend of a rise in uptake as the temperatures are

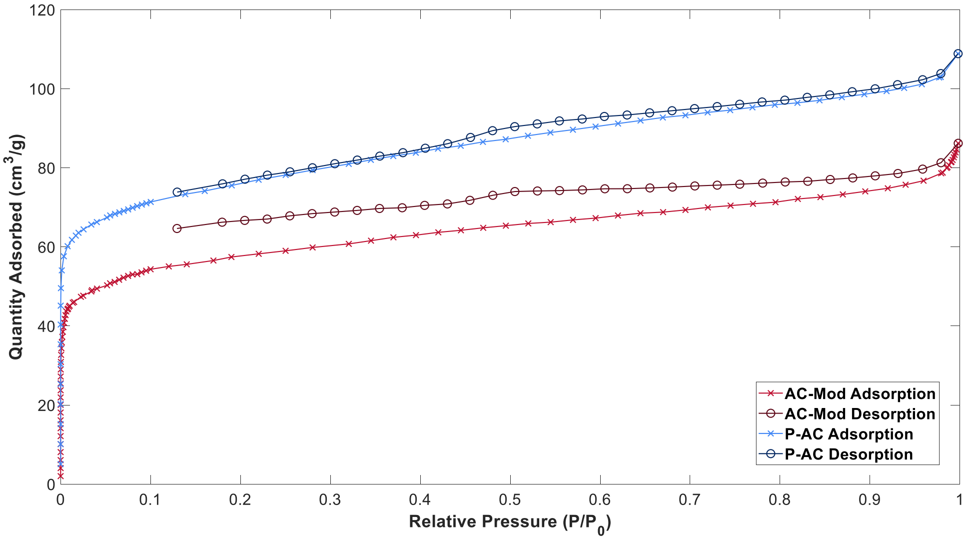

Fig. 9. BET physisorption isotherms of AC-Mod (red; bottom) and P-AC (blue; top).

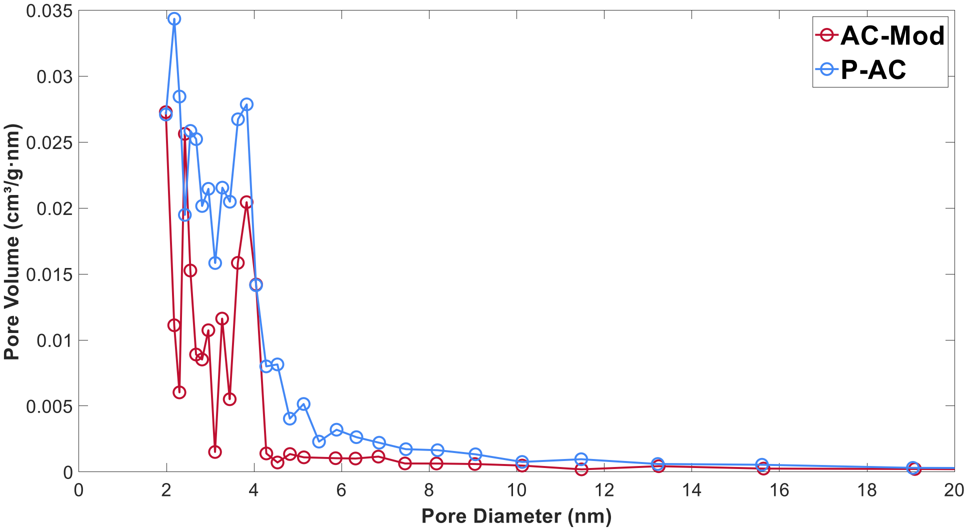

Fig. 10. Pore size distribution plots of AC-Mod (red; bottom) and P-AC (blue; top).

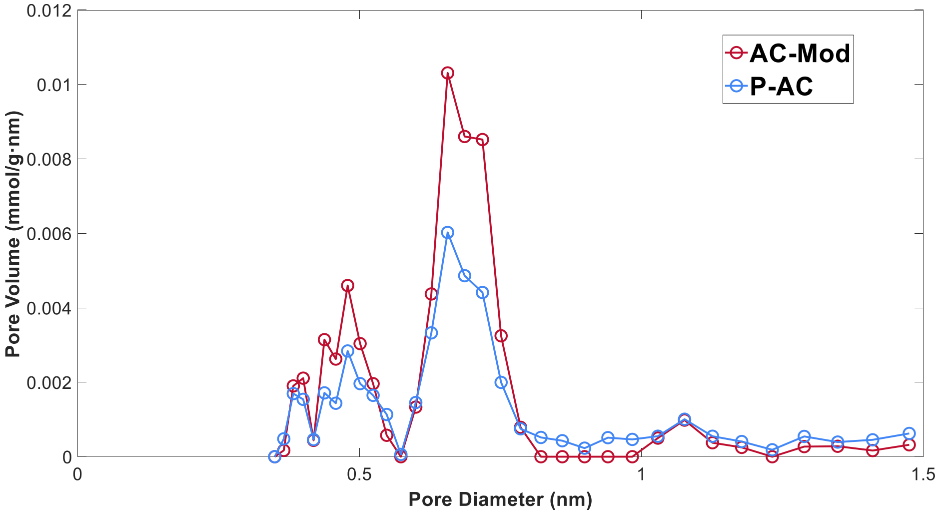

Fig. 11. Micropore size distribution plots of AC-Mod (red) and P-AC (blue).

lowered. These trends can be noted across the realm of biomass combustion ash-based sorbents [45,46].This is indicated in Table 6, which presents the uptake values acquired gravimetrically. The values of 50 °C and 75 °C were used as they are representative of post-combustion carbon capture conditions, whereas 25 °C was used as a standard temperature that is used for comparison to other adsorbents in Table 7.

The proposed modification facilitated a ~35 % rise in adsorption capacity across the evaluated temperature range, hence, outperforming a commercial analogue [15], yet is modest in comparison to other biomass combustion ash-based sorbents as well as alternative more elaborate carbonaceous adsorbents (as presented in Table 7).

Similar increases in adsorption capacity (~45 %) have previously been reported upon grafting NO_2 groups onto UiO-66 [24]. In the case of AC-Mod, however, this may be attributed to not only the grafted SFGs but also the purification (i.e. dissolution of ash) aspect described in Section 3.2.6.1.

3.3.6.3. *Equilibrium adsorption isotherms.*

Table 8 presents the *goodness of fit* for various equilibrium CO_2 adsorption isotherms for AC-Mod at 0 °C. In order to discern between the models and select the option with best fit, the R^2 and normalised root mean square error (NRMSE) were employed.

The Tri-site Langmuir model was determined to provide the best fit for the examined data (high R^2 and minimal NRMSE), although both Toth and Bi-site Langmuir models closely follow. However, it is important to mention that a higher number of fitting parameters also potentially contributes to the better fit of this model (due to overfitting). Regardless, AC-Mod is believed to possess a highly heterogenous surface morphology with a plethora of pore sizes and shapes (as evidenced by the high quality of fit for the aforementioned isotherms). Nevertheless, the values for the Tri-site Langmuir isotherm parameters are shown in Table 9, while

Fig. 12 illustrates a comparison between the model fitting and the experimental data.

The variations in active adsorption sites can be attributed to not only the variety of pore shapes and sizes (which may stem from P-AC) but also different surface functionalities originating from the acidic treatment. These, potentially, lead to a variety of different physical adsorption mechanisms (e.g. micropore filling as well as capillary condensation) for CO_2 on AC-Mod.

3.3.6.4. *Adsorption kinetics.*

A myriad of kinetic models (as per our previous work [46]) has also employed to evaluate the interaction of CO_2 and AC-Mod. Firstly, since the worst fits are provided by the intraparticle diffusion models and the Pseudo-First Order (PFO), adsorption is not diffusion-controlled [52–54]. The generated active adsorption sites (*via* activation and modification) are believed to have a more pronounced impact on the process, which is corroborated by the best fit of the Pseudo-Second Order (PSO) and the modified Ritchie models. The results of the kinetic model fitting are presented in Table 10.

Between the two models, the Modified Ritchie equation is considered to have a better fit. Hence, this model is presented in Fig. 13 and Table 11.

The more accurate fit of the Modified Ritchie model (as in the case of the Tri-site Langmuir) may arise from an additional fitting parameter, i.e. the model term associated with initial particle loading. On the other hand, this may suggest AC-Mod to not have been completely purged prior to the test.

Table 6
Results of AC-Mod CO_2 adsorption tests at different temperatures (pure CO_2 flow).

Uptake at 25 °C, mmol/g	Uptake at 50 °C, mmol/g	Uptake at 75 °C, mmol/g
1.39	0.96	0.61

Table 7
Comparison of CO_2 uptakes between AC-Mod and other samples (1 bar at 25 °C).

Sample		Uptake, mmol/g	Reference
Biomass combustion bottom ash-derived AC	Chemically Modified	1.39	This work
	Chemically Activated	1.93	[46]
	Physically Activated	1.04	[15]
Commercial AC		1.23	[15]
		1.88	[47]
S-doped coconut-shell-derived chemically activated carbon		2.86 – 3.59	[48]
Disodium 2,6-naphthalene disulfonate-derived self-S-doped porous carbon		1.76 – 2.36	[49]
Chitosan-derived chemically activated carbon		3.56 – 4.40	[50]
Biomass combustion fly ash-derived zeolite		2.27	[51]

Table 8
Equilibrium isotherm models fitted to experimental data at 0 °C (AC-Mod).

Isotherm Model	R^2	NRMSE
Langmuir	0.9813	0.1168
Freundlich	0.9876	0.0124
Bi-site Langmuir	0.9998	0.0050
Tri-site Langmuir	0.9999	0.0017
Toth	0.9999	0.0026

Table 9
AC-Mod equilibrium adsorption isotherm models' parameters at 0 °C.

Temperature	Isotherm Model	Identified Parameters	
0 °C	Tri-site Langmuir	$q_{max(1)} = 91.23$ mg/g	$K_{L\ (1)} = 0.9663$ 1/bar
		$q_{max(2)} = 11.73$ mg/g	$K_{L\ (2)} = 157.6$ 1/bar
		$q_{max(3)} = 54.05$ mg/g	$K_{L\ (3)} = 14.39$ 1/bar

3.3.6.5. *Adsorption working capacity.*

Cyclic adsorption-desorption studies have also been employed to envisage the working capacity of AC-Mod (Fig. 14).

As anticipated, a decline in adsorption loading is evident after the first cycle. After exposure of an adsorbent to a stream of pure CO_2, the highest energy sites may not desorb completely, reducing the capacity from the first cycle to the second. Consequently, AC-Mod adsorbed 2 % less during the second adsorption test. This observation highlights the significance of such studies. Subsequently, another 2 % of uptake was lost in cycle three. After cycle four until cycle 40 (end of observation), fractional coverage (θ) fluctuated between 0.95 and 0.96.

One possible explanation for these fluctuations could be incomplete desorption (as proposed by the best fit of Modified Ritchie equation) of various heterogeneous adsorption sites (as per the Tri-site Langmuir fit) with different adsorption energies (discussed in the following section). Alternatively, slight changes in ambient conditions and/or instrument error may have also impacted the observed minor fluctuations.

Nevertheless, AC-Mod acts in a manner, similar to the parent AC-Mod, maintaining a high fractional loading even after 40 adsorption-desorption cycles, whereas a chemically activated analogue reaches end of its work-life (i.e. $\theta = 0.85$) after the same number of steps [46]. In addition, AC-Mod presents a significantly lesser decrease in capacity than alternative amine-functionalised zeolitic [55] and silicas [56,57] and ACs (both modified [14] and non-modified [58]) adsorbents, underlying the advantage of the method employed in this work over the existing reports in the scientific domain.

3.3.6.6. *Heat of adsorption.*

The isosteric heat of adsorption is a

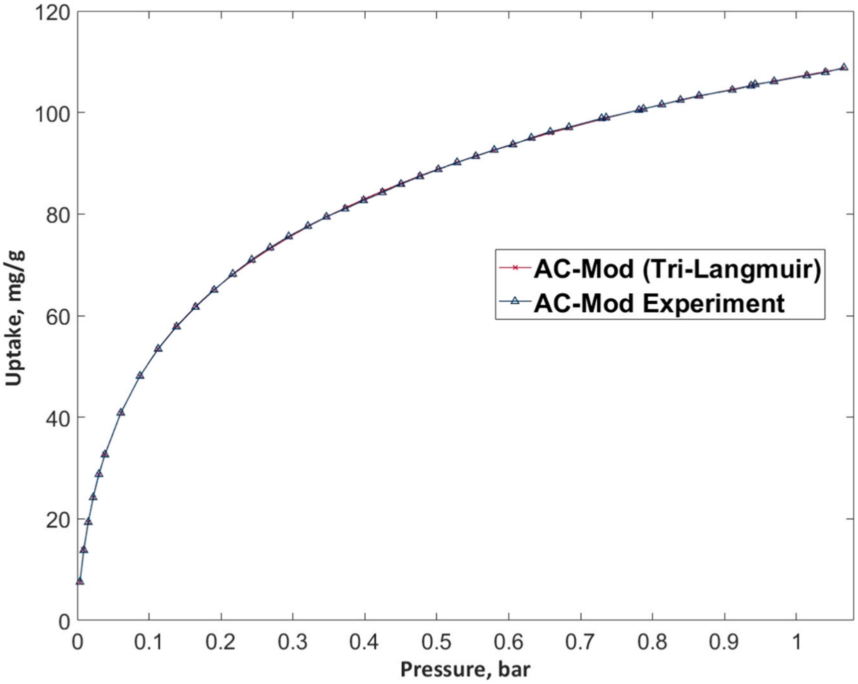

Fig. 12. Experimental data (blue triangles) and the equilibrium isotherm model (red crosses) for AC-Mod at 0 °C under pure CO_2.

Table 10
CO_2 adsorption kinetic model fits for AC-Mod at 50 ºC (flow rate: 50 mL/min).

Kinetic Model	R^2	NRMSE
Pseudo-First Order (PFO)	0.6526	0.0869
Pseudo-Second Order (PSO)	0.9838	0.0188
Modified Ritchie	0.9843	0.0185
Intraparticle diffusion	0.6608	0.0858
Avrami	0.9595	0.0297
Elovich	0.9093	0.0444

valuable metric when selecting adsorbents as it is directly related to the amount of energy required for regeneration, hence, the energy penalty of CO_2 separation. Therefore, it should not be overlooked. The procedure for obtaining this value is described in our previous work [46]. Briefly, a number of isotherms at different temperatures are required as inputs to the Clausius-Clapeyron equation (Eq. 3) to produce a curve displaying the heat of adsorption as a function of uptake *or* loading. Fig. 15 illustrates the plot obtained for AC-Mod.

$$Q_{st} = -R\left[\partial \ln p \Big/ \partial\left(\frac{1}{T}\right)\right]_{q_e} \tag{3}$$

As anticipated, the heat of adsorption decreases with an increase in CO_2 uptake. This is linked to occupation of low energy sites, i.e. conditions of bulk adsorption. For AC-Mod, this trend continues until the

Table 11
CO_2 adsorption kinetics on AC-Mod at 50 ºC.

Kinetic Model	Identified Parameters
Modified Ritchie	$K_{(R)} = 0.02264$ β= 1.155

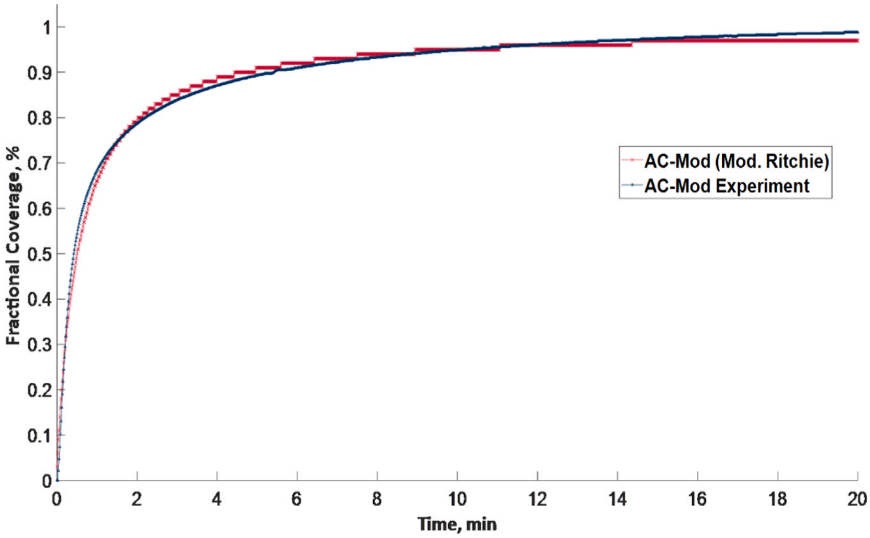

Fig. 13. Experimental data (blue triangles) and the kinetic model (red crosses) for pure CO_2 adsorption on AC-Mod at 50 °C and 1 bar.

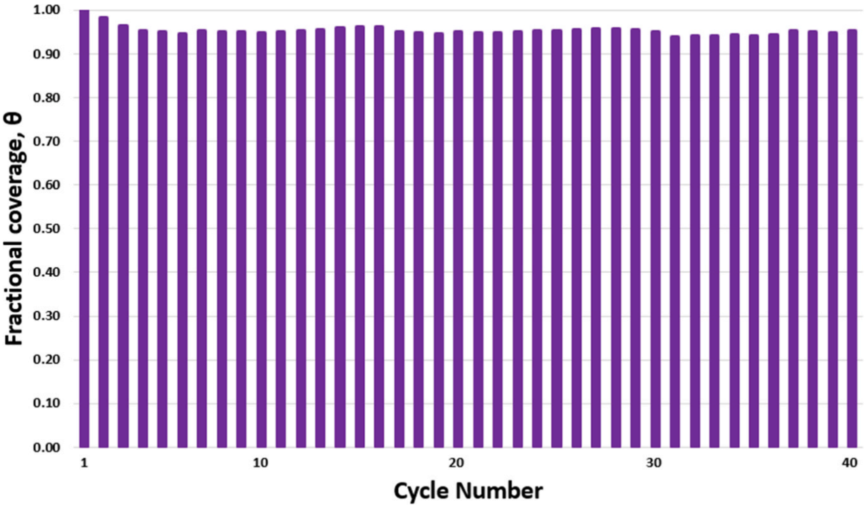

Fig. 14. Working capacity of AC-Mod over 40 adsorption-desorption cycles.

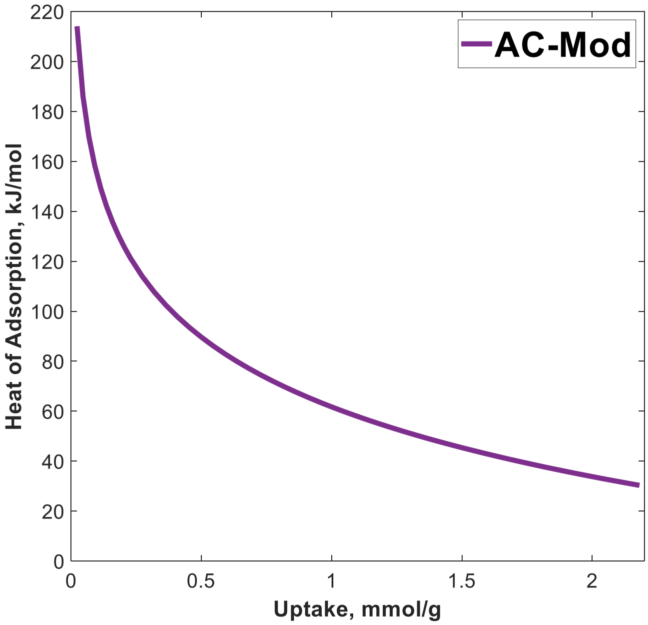

Fig. 15. Heat of CO_2 adsorption on AC-Mod.

uptake of 2.18 mmol/g, where the heat of adsorption is calculated to be 30.5 kJ/mol. This constitutes a notable increase from P-AC (26.5 kJ/mol) suggesting the generated functionalities to increase the affinity towards CO_2.

Moreover, as discussed in Section 3.2.6.5, the observed relatively strong decline in cyclic capacity of AC-Mod from the first cycle to the second is in line with a high isosteric heat of adsorption values at/near zero coverage as can be seen in Fig. 15. These would suggest the high energy adsorption site to possess a very strong affinity towards CO_2; preventing full regeneration of the sorbent, hence, declines during the consecutive cycle steps.

Generally, final/bulk isosteric heat of adsorption values below 40 kJ/mol are ascribed to physical adsorption, whilst high values (>80 kJ/mol) often stem from chemical interactions with the adsorbate (i.e. chemical bonding). However, this indicator on its own is not sufficient to ascribe chemisorption (as it merely describes high affinity between the adsorbate and the adsorption site) and, in the case of AC-Mod, it is not the case as no functional groups with the ability to form substrates with CO_2 were noted (Section 3.2.4.1). Further, zero loading heat of adsorption is notoriously known to be less accurate compared to bulk adsorption as there are less data points collected [59]. Nevertheless, the higher values at the initial stages of adsorption are believed to be culpable for the drop in working capacity.

4. Conclusion and future work

An acidic (H_2SO_4 and HNO_3) surface modification technique of a biomass combustion ash-based physically activated carbon has been investigated. This campaign aimed to introduce novel functional groups (namely, nitro groups) and investigate their impact onto the interaction between CO_2 and the sorbent. The experiments were conducted based on a randomised Box-Behnken design (four parameters at three levels each). As a result of the optimisation campaign, the reaction temperature and the individual concentrations of the employed acids were found to have statistically pronounced effects, whilst the CO_2 uptake was maximised under the following modification conditions: 3-hour treatment at 90 °C with 1:2 HNO_3/H_2SO_4 volumetric ratio 1 molar acid mixture.

As a result of such surface modification, an enhanced affinity towards CO_2 was noted as evidenced by a larger adsorption capacity (0.96 mmol/g at 50 °C) as well as a greater heat of adsorption (30.5 kJ/mol). This was ascribed to a combination of AC purification *via* dissolution of ash impurities as well as the impact of the introduced functional groups. The former was evidenced by proximate analysis, whereas the latter was corroborated by FTIR spectroscopy and ultimate analysis. Further, the modified adsorbent has a high working capacity: losing no more than 5 % of the original uptake value over 40 adsorption-desorption cycles.

The proposed modification outlines a more facile and cost-effective route as opposed to amine grafting, i.e. the conventional approach. However, this modification is not without its limitations. For instance, the CO_2 adsorption capacity of the modified sample falls short of the conventional benchmark of 2 mmol/g at 25 °C. Additionally, the elevated moisture content (compared to the parent AC) suggests the sample to be potentially fallible to competitive (H_2O and CO_2) adsorption. Finally, although this modification approach avoids usage of harmful reducing agents, the co-generation of brown NO_2 gas is a further limitation of this modification technique (requiring the synthesis procedure to be conducted with strong fumes extraction procedures to be in place).

Further work could explore introduction of alternative heteroatoms (e.g. S or P) *via* respective pure acids. Such investigations may also deploy the presence/quantity of the desired species (functional groups or heteroatom) as the dependent variable to provide insight into the reaction between the sorbent and modifier. Alternatively, based on the results of this experimental campaign, two potential avenues for exploration may be of interest. Firstly, since the optimum point was found to be on the corner of the design space, adjusting the levels of the studied factors (to incorporate the current edge-point into the internal volume of the design framework) may allow to further optimise this modification procedure. Alternatively, future work may look into minimising energy costs of the proposed treatment by decreasing the temperature and time. This approach, however, may not modify the sorbent but only dissolve the ash species, hence, act as a purification step. Finally, investigations into impacts of moisture onto the CO_2 adsorption of such functionalised samples would be of practical benefit for applications under a real flue gas stream.

Author contribution statement

MG (first/lead Author) Writing (Original Draft & Editing), Conceptualisation, Methodology, Investigation, Formal Analysis, Validation, Visualisation; **LHP (2nd/contributing author)**: Writing (Original Draft), Visualisation, Investigation, Validation, Formal Analysis; **SI (3rd/contributing author)** Resources, Supervision; **PH (4th/contributing author)** Resources, Supervision; **SMS (corresponding author)**: Supervision, Funding Acquisition, Writing (Review & Editing), Resources, Conceptualisation, Project Administration.

Declaration of Competing Interest

The authors declare that they have no known competing financial interests or personal relationships that could have appeared to influence the work reported in this paper.

Acknowledgements

This work has been funded by the UK Carbon Capture and Storage Research Centre (EP/W002841/1) through the flexible funded research programme “Investigation of Environmental and Operational Challenges of Adsorbents Synthesised from Industrial Grade Biomass Combustion Residues”. The UKCCSRC is supported by the Engineering and Physical Sciences Research Council (EPSRC), UK, as part of the UKRI Energy Programme.

The authors would like to thank and acknowledge the Experimental Techniques Centre (ETC) at Brunel University London and their scientific officers (namely, Dr Ashley Howkins, Dr Myles Worsley, Dr Nicholas Nelson and Dr Uche Onwukwe) for facilitating access to analytical equipment.

The authors would like to recognise Sebastien Genta from IUT Paul Sabatier University of Toulouse III for facilitating this collaboration.

Last but not least, we would also like to acknowledge the continued generous support from Drax Group UK, with a special thanks to Dr James Hammerton throughout this research.

References

[1] S. Sircar, Pressure swing adsorption, Ind. Eng. Chem. Res [Internet] 41 (6) (2002) 1389–1392. Available from: https://pubs.acs.org/doi/10.1021/ie0109758.

[2] A.E. Rodrigues, Chemical engineering and environmental challenges. Cyclic adsorption/reaction technologies: Materials and process together!, J. Environ. Chem. Eng. [Internet] 8 (4) (2020) 103926, https://doi.org/10.1016/j.jece.2020.103926.

[3] A. Houshmand, W.M.A.W. Daud, M.S. Shafeeyan, Exploring potential methods for anchoring amine groups on the surface of activated carbon for CO2 adsorption, Sep Sci. Technol. 46 (7) (2011) 1098–1112.

[4] T. Li, B. Huang, S. Wang, C. Chen, L. Tang, Q. Lu, et al., Covalent grafting of organic molecules onto activated carbon by a single step, Bioresour. [Internet] 8 (2) (2013) 2300–2309 (Available from: https://bioresources.cnr.ncsu.edu/resources/covalent-grafting-of-organic-molecules-onto-activated-carbon-by-a-single-step/).

[5] Y. Miao, Z. He, X. Zhu, D. Izikowitz, J. Li, Operating temperatures affect direct air capture of CO2 in polyamine-loaded mesoporous silica, Chem. Eng. J. [Internet] 426 (2021) 131875. Available from: https://linkinghub.elsevier.com/retrieve/pii/S1385894721034525.

[6] G. Rim, F. Kong, M. Song, C. Rosu, P. Priyadarshini, R.P. Lively, et al., Sub-Ambient Temperature Direct Air Capture of CO 2 using Amine-Impregnated MIL-101(Cr) Enables Ambient Temperature CO 2 Recovery, JACS Au [Internet] 2 (2) (2022) 380–393. ⟨https://pubs.acs.org/doi/10.1021/jacsau.1c00414⟩ (Available from:).

[7] D. Panda, S.K. Singh, E.A. Kumar, A comparative study of CO2 capture by amine grafted vs amine impregnated zeolite 4A, IOP Conf. Ser. Mater. Sci. Eng. [Internet] 377 (2018 Jun) 012148. ⟨https://iopscience.iop.org/article/10.1088/1757-899X/377/1/012148⟩ (Available from:).

[8] F. Liu, T. Wang, H. Dong, W. Liu, Modified metal–organic framework by a novel coordinatively unsaturated amine grafting mechanism for direct air capture of CO2, Chem. Eng. J. [Internet] 454 (2023 Feb) 140431. ⟨https://linkinghub.elsevier.com/retrieve/pii/S1385894722059113⟩ (Available from:).

[9] J.J. Lee, C.-H. Chen, D. Shimon, S.E. Hayes, C. Sievers, C.W. Jones, Effect of Humidity on the CO2 Adsorption of Tertiary Amine Grafted SBA-15, J. Phys. Chem. C. [Internet] 121 (42) (2017) 23480–23487. ⟨https://pubs.acs.org/doi/10.1021/acs.jpcc.7b07930⟩ (Available from:).

[10] M. Jahandar Lashaki, A. Sayari, CO2 capture using triamine-grafted SBA-15: the impact of the support pore structure, Chem. Eng. J. [Internet] 334 (2018 Feb) 1260–1269. ⟨https://linkinghub.elsevier.com/retrieve/pii/S1385894717318193⟩ (Available from).

[11] A. Justin, J. Espín, M.J. Pougin, D. Stoian, T. Schertenleib, M. Mensi, et al., Post-synthetic covalent grafting of Amines to NH 2 -MOF for post-combustion carbon capture, Adv. Funct. Mater. [Internet] (2023). ⟨https://onlinelibrary.wiley.com/doi/10.1002/adfm.202307430⟩ (Available from:).

[12] B. Wadi, A. Golmakani, V. Manovic, S.A. Nabavi, Effect of combined primary and secondary amine loadings on the adsorption mechanism of CO2 and CH4 in biogas, Chem. Eng. J. [Internet] 420 (2021 Sep) 130294. ⟨https://linkinghub.elsevier.com/retrieve/pii/S1385894721018817⟩ (Available from:).

[13] M. Keramati, A.A. Ghoreyshi, Improving CO2 adsorption onto activated carbon through functionalization by chitosan and triethylenetetramine, Phys. E Low. Dimens. Syst. Nanostruct. [Internet] 57 (2014 Mar) 161–168. ⟨https://linkinghub.elsevier.com/retrieve/pii/S1386947713003524⟩ (Available from).

[14] A. Houshmand, M.S. Shafeeyan, A. Arami-Niya, W.M.A.W. Daud, Anchoring a halogenated amine on the surface of a microporous activated carbon for carbon dioxide capture, J. Taiwan Inst. Chem. Eng. 44 (5) (2013) 774–779.

[15] M. Gorbounov, B. Petrovic, S. Ozmen, P. Clough, S. Masoudi Soltani, Activated carbon derived from Biomass combustion bottom ash as solid sorbent for CO2 adsorption, Chem. Eng. Res Des. [Internet] 194 (2023 Jun) 325–343, https://doi.org/10.1016/j.cherd.2023.04.057.

[16] S. Masoudi Soltani, S.K. Yazdi, S. Hosseini, M.K. Gargari, Effect of nitric acid modification on porous characteristics of mesoporous char synthesized from the pyrolysis of used cigarette filters, J. Environ. Chem. Eng. 2 (3) (2014) 1301–1308.

[17] W. Somyanonthanakun, R. Ahmed, V. Krongtong, S. Thongmee, Studies on the adsorption of Pb(II) from aqueous solutions using sugarcane bagasse-based modified activated carbon with nitric acid: Kinetic, isotherm and desorption, Chem. Phys. Impact [Internet] 6 (2023 Jun) 100181. ⟨https://linkinghub.elsevier.com/retrieve/pii/S266702242300021X⟩ (Available from:).

[18] Demiral İ., Samdan C., Demiral H. Enrichment of the surface functional groups of activated carbon by modification method. Surfaces and Interfaces [Internet]. 2021 Feb;22:100873. Available from: https://linkinghub.elsevier.com/retrieve/pii/S2468023020308658.

[19] M. Gorbounov, J. Taylor, B. Petrovic, Masoudi, S. Soltani, To DoE or not to DoE? A technical review on & roadmap for optimisation of carbonaceous adsorbents and adsorption processes, South Afr. J. Chem. Eng. [Internet] 41 (July) (2022 Jul) 111–128. ⟨https://linkinghub.elsevier.com/retrieve/pii/S1026918522000385⟩.

[20] M.R. Ketabchi, S. Babamohammadi, W.G. Davies, M. Gorbounov, S. Masoudi Soltani, Latest advances and challenges in carbon capture using bio-based sorbents: a state-of-the-art review, Carbon Capture Sci. Technol. [Internet] 6 (October 2022) (2023 Mar) 100087, https://doi.org/10.1016/j.ccst.2022.100087.

[21] J.H. Taylor, S. Masoudi Soltani, Carbonaceous adsorbents in the removal of aquaculture pollutants: a technical review of methods and mechanisms (Available from:), Ecotoxicol. Environ. Saf. [Internet] 266 (September) (2023 Nov) 115552, https://doi.org/10.1016/j.ecoenv.2023.115552.

[22] B. Petrovic, M. Gorbounov, S. Masoudi Soltani, Impact of surface functional groups and their introduction methods on the mechanisms of CO2 adsorption on porous carbonaceous adsorbents, Carbon Capture Sci. Technol. [Internet] 3 (2022 Jun) 100045. ⟨https://linkinghub.elsevier.com/retrieve/pii/S2772656822000161⟩.

[23] B. Petrovic, M. Gorbounov, S. Masoudi Soltani, Influence of surface modification on selective CO2 adsorption: A technical review on mechanisms and methods, Microporous Mesoporous Mater. [Internet] 312 (September 2020) (2021 Jan) 110751, https://doi.org/10.1016/j.micromeso.2020.110751.

[24] G.E. Cmarik, M. Kim, S.M. Cohen, K.S. Walton, Tuning the adsorption properties of uio-66 via ligand functionalization, Langmuir 28 (44) (2012) 15606–15613.

[25] Y. He, X. Zhu, Y. Li, C. Peng, J. Hu, H. Liu, Efficient CO2 capture by triptycene-based microporous organic polymer with functionalized modification, Microporous Mesoporous Mater. 214 (2015) 181–187.

[26] ASTM. ASTM D3172–13, Standard Practice for Proximate Analysis of Coal and Coke [Internet]. West Conshohocken, PA, USA; 2013. Available from: https://www.astm.org/Standards/D3172.htm.

[27] S. Brunauer, P.H. Emmett, E. Teller, Adsorption of gases in multimolecular layers, J. Am. Chem. Soc. [Internet] 60 (2) (1938) 309–319. ⟨https://pubs.acs.org/doi/abs/10.1021/ja01269a023⟩ (Available from:).

[28] M.S. Shafeeyan, A. Houshmand, A. Arami-Niya, H. Razaghizadeh, W.M.A.W. Daud, Modification of activated carbon using nitration followed by reduction for carbon dioxide capture, Bull. Korean Chem. Soc. 36 (2) (2015) 533–538.

[29] G. Zhang, S. Sun, D. Yang, J.-P. Dodelet, E. Sacher, The surface analytical characterization of carbon fibers functionalized by H2SO4/HNO3 treatment, Carbon N. Y 46 (2) (2008 Feb) 196–205.

[30] T. Dahiru, P-Value, a true test of statistical significance? A cautionary note, Ann. Ib. Post. Med [Internet] 6 (1) (2008 Mar 3) 21–26. ⟨http://www.ajol.info/index.php/aipm/article/view/64038⟩ (Available from:).

[31] M.L. Head, L. Holman, R. Lanfear, A.T. Kahn, M.D. Jennions, The extent and consequences of P-hacking in science, PLOS Biol. [Internet] 13 (3) (2015) e1002106. ⟨https://dx.plos.org/10.1371/journal.pbio.1002106⟩.

[32] T. Dahiru, P-Value, a true test of statistical significance? A cautionary note, Ann. Ib. Post. Med 6 (1) (2008) 21–26 (Mar).

[33] M.L. Head, L. Holman, R. Lanfear, A.T. Kahn, M.D. Jennions, The extent and consequences of p-hacking in science, PLOS Biol. 13 (3) (2015 Mar) e1002106.

[34] J.-H. Kim, S.Y. Hwang, J.E. Park, G.B. Lee, H. Kim, S. Kim, et al., Impact of the oxygen functional group of nitric acid-treated activated carbon on KOH activation reaction, Carbon Lett. 29 (3) (2019 Jun) 281–287.

[35] J.J. Ternero-Hidalgo, J.M. Rosas, J. Palomo, M.J. Valero-Romero, J. Rodríguez-Mirasol, T. Cordero, Functionalization of activated carbons by HNO3 treatment: influence of phosphorus surface groups, Carbon N. Y 101 (2016 May) 409–419.

[36] J. Konopka, Options for quantitative analysis of light elements by SEM/EDS [Internet]. Thermo Fisher Scientific Technical Note 52523. Madison, WI (2013) 1–4. ⟨https://assets.thermofisher.com/TFS-Assets/CAD/Warranties/TN52523_E_0713M_LightElement_H.pdf⟩.

[37] Merck. I.R. Spectrum Table & Chart [Internet]. 2023 [cited 2023 Jun 13]. Available from: https://www.sigmaaldrich.com/GB/en/technical-documents/technical-article/analytical-chemistry/photometry-and-reflectometry/ir-spectrum-table.

[38] J.H. Taylor, G. Troisi, S.M. Soltani, Application of chemically-activated recycled carbon fibres for aqueous-phase adsorptions - part I: optimisation of activation process, Chem. Eng. J. Adv. [Internet] (2024 Feb) 100591. ⟨https://linkinghub.elsevier.com/retrieve/pii/S2666821124000097⟩ (Available from:).

[39] University of Toronto (TRACES Centre). Understanding Raman Spectroscopy. Principles and Theory [Internet]. 2021. Available from: https://www.utsc.utoronto.ca/~traceslab/PDFs/raman_understanding.pdf.

[40] K. Krishnan, Raman spectra of organic compounds, Proc. Indian Acad. Sci. Sect. A [Internet] 54 (2) (1961 Aug) 89–98. ⟨http://link.springer.com/10.1007/BF03047404⟩ (Available from:).

[41] Rouquerol J., Rouquerol F., Llewellyn P., Maurin G., Sing K.S.W. Adsorption by Powders and Porous Solids: Principles, Methodology and Applications: Second Edition. Adsorption by Powders and Porous Solids: Principles, Methodology and Applications: Second Edition. 2013. 1–626 p.

[42] P. Maziarka, P. Sommersacher, X. Wang, N. Kienzl, S. Retschitzegger, W. Prins, et al., Tailoring of the pore structures of wood pyrolysis chars for potential use in energy storage applications, Appl. Energy [Internet] 286 (2021 Mar) 116431. ⟨https://linkinghub.elsevier.com/retrieve/pii/S030626192031792X⟩ (Available from:).

[43] W.J. Braida, J.J. Pignatello, Y. Lu, P.I. Ravikovitch, A.V. Neimark, B. Xing, Sorption hysteresis of benzene in charcoal particles, Environ. Sci. Technol. [Internet] 37 (2) (2003 Jan 1) 409–417. ⟨https://pubs.acs.org/doi/10.1021/es020660z⟩.

[44] C. Wedler, R. Span, Micropore analysis of biomass chars by CO2 adsorption: comparison of different analysis methods, Energy Fuels 35 (10) (2021) 8799–8806.

[45] Gorbounov M., Petrovic B., Ozmen S., Clough P., Bekmuratova D., Soltani S.M. Development of Nanoporosity on a Biomass Combustion Ash-derived Carbon for CO2 Adsorption. In: 2022 IEEE 22nd International Conference on Nanotechnology (NANO) [Internet]. IEEE; 2022. p. 245–8. Available from: https://ieeexplore.ieee.org/document/9928660/.

[46] M. Gorbounov, E. Diaz-Vasseur, D. Danaci, S. Masoudi Soltani, Chemical activation of porous carbon extracted from biomass combustion bottom ash for CO2 adsorption, Carbon Capture Sci. Technol. [Internet] 10 (October 2023) (2024 Mar) 100151, https://doi.org/10.1016/j.ccst.2023.100151.

[47] N.A. Rashidi, S. Yusup, Co-valorization of delayed petroleum coke – palm kernel shell for activated carbon production, J. Hazard Mater. [Internet] 403 (2021 Feb) 123876. ⟨https://linkinghub.elsevier.com/retrieve/pii/S0304389420318653⟩.

[48] J. Bai, J. Shao, Q. Yu, M. Demir, B. Nazli Altay, T. Muhammad Ali, et al., Sulfur-Doped porous carbon Adsorbent: A promising solution for effective and selective CO2 capture, Chem. Eng. J. [Internet] 479 (2024 Jan) 147667. ⟨https://linkinghub.elsevier.com/retrieve/pii/S1385894723063994⟩ (Available from:).

[49] T. Lu, J. Bai, J. Huang, Q. Yu, M. Demir, M. Kilic, et al., Self-Activating Approach for Synthesis of 2,6-Naphthalene Disulfonate Acid Disodium Salt-Derived Porous Carbon and CO 2 Capture Performance, Energy Fuels [Internet] 37 (5) (2023 Mar 2) 3886–3893. ⟨https://pubs.acs.org/doi/10.1021/acs.energyfuels.2c04320⟩ (Available from:).

[50] J. Shao, J. Wang, Q. Yu, F. Yang, M. Demir, O.C. Altinci, et al., Unlocking the potential of N-doped porous Carbon: Facile synthesis and superior CO2 adsorption performance, Sep Purif. Technol. [Internet] 333 (2024 Apr) 125891. ⟨https://linkinghub.elsevier.com/retrieve/pii/S1383586623027995⟩ (Available from:).

[51] B. Petrovic, M. Gorbounov, S. Masoudi Soltani, Synthesis of biomass combustion fly ash derived zeolites for CO2 adsorption: Optimisation of hydrothermal synthetic pathway, Carbon Capture Sci. Technol. [Internet] 12 (June)) (2024 Sep) 100245. ⟨https://linkinghub.elsevier.com/retrieve/pii/S2772656824000575⟩ (Available from:).

[52] S. Masoudi Soltani, S. Kazemi Yazdi, S. Hosseini, I. Bayestie, Lead removal from aqueous solution using non-modified and nitric acid-modified charred carbon from the pyrolysis of used cigarette filters, Desalin. Water Treat. [Internet] 53 (1) (2015 Jan 2) 126–138. ⟨http://www.tandfonline.com/doi/abs/10.1080/19443994.2013.835751⟩ (Available from:).

[53] J. Wang, X. Guo, Adsorption kinetic models: physical meanings, applications, and solving methods (Available from:), J. Hazard Mater. [Internet] 390 (November 2019) (2020) 122156, https://doi.org/10.1016/j.jhazmat.2020.122156.

[54] Gorbounov M., Diaz-Vasseur E., Panek R., Soltani S.M. Impact of Production Pathway on Nanoporosity of Carbonaceous Sorbents for CO 2 Adsorption. In: 2023 IEEE 23rd International Conference on Nanotechnology (NANO) [Internet]. IEEE; 2023. p. 249–54. Available from: https://ieeexplore.ieee.org/document/10231299/.

[55] C. Kim, H.S. Cho, S. Chang, S.J. Cho, M. Choi, An ethylenediamine-grafted Y zeolite: a highly regenerable carbon dioxide adsorbent via temperature swing adsorption without urea formation, Energy Environ. Sci. [Internet] 9 (5) (2016) 1803–1811. Available from: http://xlink.rsc.org/?DOI=C6EE00601A.

[56] E.S. Sanz-Pérez, M. Olivares-Marín, A. Arencibia, R. Sanz, G. Calleja, M.M. Maroto-Valer, CO2 adsorption performance of amino-functionalized SBA-15 under post-combustion conditions, Int J. Greenh. Gas. Control [Internet] 17 (2013 Sep) 366–375. Available from: https://linkinghub.elsevier.com/retrieve/pii/S1750583613002144.

[57] D.S. Dao, H. Yamada, K. Yogo, Enhancement of CO2 adsorption/desorption properties of solid sorbents using tetraethylenepentamine/diethanolamine blends, ACS Omega [Internet] 5 (37) (2020) 23533–23541. ⟨https://pubs.acs.org/doi/10.1021/acsomega.0c01515⟩ (Available from:).

[58] Y.-F. Huang, P.-T. Chiueh, C.-H. Shih, S.-L. Lo, L. Sun, Y. Zhong, et al., Microwave pyrolysis of rice straw to produce biochar as an adsorbent for CO2 capture, Energy [Internet] 84 (2015 May) 75–82. ⟨https://linkinghub.elsevier.com/retrieve/pii/S0360544215001814⟩ (Available from).

[59] A. Nuhnen, C. Janiak, A practical guide to calculate the isosteric heat/enthalpy of adsorption via adsorption isotherms in metal–organic frameworks, MOFs, Dalt Trans. 49 (30) (2020) 10295–10307. ⟨http://xlink.rsc.org/?DOI=D0DT01784A⟩ (Available from:).